

Simulation of Shallow-water Flows in Complex Bay-like Domains

Yuri N. Skiba¹ and Denis M. Filatov²

¹Centre for Atmospheric Sciences (CCA), National Autonomous University of Mexico (UNAM),
Av. Universidad 3000, C.P. 04510, Mexico City, Mexico

²Centre for Computing Research (CIC), National Polytechnic Institute (IPN),
Av. Juan de Dios Batiz s/n, C.P. 07738, Mexico City, Mexico

Keywords: Simulation of Fluid Dynamics Problems, Shallow-water Flows, Conservative Finite Difference Schemes, Complex Computational Domain, Closed and Open Boundaries.

Abstract: A new numerical method for the simulation of shallow-water flows in a bay-like domain is suggested. The method is based on the splitting of the original nonlinear operator by physical processes and by coordinates. An essential advantage of our finite difference splitting-based method versus others in the field is that it leads to a model allowing accurate simulation of shallow-water flows in a domain of an arbitrary shape with both closed and open boundaries, which besides may contain onshore parts inside (interior isles in the bay); the model also takes into account irregular bottom topography. Specially constructed approximations of the temporal and spatial derivatives result in second-order unconditionally stable finite difference schemes that conserve the mass and the total energy of the discrete inviscid unforced shallow-water system. Moreover, the potential enstrophy results to be bounded, oscillating in time within a narrow range. Therefore, the numerical solution, aside from being accurate from the mathematical point of view, appears to be physically adequate, inheriting a number of substantial properties of the original differential shallow-water system. Furthermore, the method can straightforwardly be implemented for distributed simulation of shallow-water flows on high-performance parallel computers. To test the method numerically, we start with the inviscid shallow-water model and verify the conservatism of the schemes in a simple computational domain. Then we introduce a domain with a more complex boundary consisting of closed and open segments, and consider more realistic viscous wind-driven shallow-water flows. Numerical experiments presented confirm the skills of the developed method.

1 INTRODUCTION

When studying a 3D fluid dynamics problem in which typical horizontal scales are much larger than the vertical ones—say, the vertical component of the velocity field is rather small compared to the horizontal ones, or horizontal movements of the fluid are normally much larger than the vertical ones—it is often useful to reduce the original problem, usually described by the Navier-Stokes equations, to a 2D approximation. This leads to a shallow-water model (Vol'tsynger and Pyaskovskiy, 1977; Pedlosky, 1987; Kundu et al., 2012).

Shallow-water equations (SWEs) naturally arise in the researches of global atmospheric circulation, tidal waves, river flows, tsunamis, among others (Jirka and Uijtewaal, 2004). In the spherical coordinates (λ, φ) the shallow-water equations for an ideal unforced fluid can be written as (Skiba and Filatov, 2009)

$$\begin{aligned} \frac{\partial U}{\partial t} + \frac{1}{R \cos \varphi} \frac{1}{2} \left[\left(\frac{\partial u U}{\partial \lambda} + u \frac{\partial U}{\partial \lambda} \right) \right. \\ \left. + \left(\frac{\partial v U \cos \varphi}{\partial \varphi} + v \cos \varphi \frac{\partial U}{\partial \varphi} \right) \right] \\ - \left(f + \frac{u}{R} \tan \varphi \right) V = - \frac{gz}{R \cos \varphi} \frac{\partial h}{\partial \lambda}, \end{aligned} \quad (1)$$

$$\begin{aligned} \frac{\partial V}{\partial t} + \frac{1}{R \cos \varphi} \frac{1}{2} \left[\left(\frac{\partial u V}{\partial \lambda} + u \frac{\partial V}{\partial \lambda} \right) \right. \\ \left. + \left(\frac{\partial v V \cos \varphi}{\partial \varphi} + v \cos \varphi \frac{\partial V}{\partial \varphi} \right) \right] \\ + \left(f + \frac{u}{R} \tan \varphi \right) U = - \frac{gz}{R} \frac{\partial h}{\partial \varphi}, \end{aligned} \quad (2)$$

$$\frac{\partial h}{\partial t} + \frac{1}{R \cos \varphi} \left[\frac{\partial z U}{\partial \lambda} + \frac{\partial z V \cos \varphi}{\partial \varphi} \right] = 0. \quad (3)$$

Here $U \equiv uz$, $V \equiv vz$, where $u = u(\lambda, \varphi, t)$ and $v = v(\lambda, \varphi, t)$ are the fluid's velocity components, $H = H(\lambda, \varphi, t)$ is the fluid's depth, $z \equiv \sqrt{H}$, $f = f(\varphi)$ is the

Coriolis acceleration due to the rotation of the sphere, R is the radius of the sphere, $h = h(\lambda, \varphi, t)$ is the free surface height, g is the gravitational acceleration. Besides, $h = H + h_T$, where $h_T = h_T(\lambda, \varphi)$ is the bottom topography. We shall study (1)-(3) in a bounded domain D on a sphere with an arbitrary piecewise smooth boundary Γ , assuming that λ is the longitude (positive eastward) and φ is the latitude (positive northward).

As we are dealing with a boundary value problem, system (1)-(3) has to be equipped with boundary conditions.

The question of imposing correct boundary conditions for SWEs is not trivial. Many independent research papers have been dedicated to this issue for the last several decades (Vol'tsynger and Pyaskovskiy, 1977; Olinger and Sundstrom, 1978; Vreugdenhil, 1994; Agoshkov and Saleri, 1996). Depending on the type of the boundary—inflow, outflow or closed—as well as on the particular physical application, one or another set of boundary conditions should be used. Following (Agoshkov and Saleri, 1996), we represent the boundary as $\Gamma = \Gamma_o \cup \Gamma_c$, where Γ_o is the open part of the boundary, while Γ_c is its closed part. Such a representation of the boundary simulates a bay-like domain, where the coastline corresponds to the closed part Γ_c , while the influence of the ocean is modelled via the open segment Γ_o . Yet, the open segment is divided into the inflow $\Gamma_{\text{inf}} := \{(\lambda, \varphi) \in \Gamma : \mathbf{n} \cdot \mathbf{u} < 0\}$ and outflow $\Gamma_{\text{out}} := \{(\lambda, \varphi) \in \Gamma : \mathbf{n} \cdot \mathbf{u} > 0\}$. Here \mathbf{n} is the outward unit normal to Γ , $\mathbf{u} = (u, v)^T$. On the closed part we put

$$\mathbf{n} \cdot \mathbf{u} = 0, \quad (4)$$

on the inflow we assume

$$\boldsymbol{\tau} \cdot \mathbf{u} = 0, \quad h = h_{(\Gamma)} \quad (5)$$

and on the outflow it holds

$$h = h_{(\Gamma)}, \quad (6)$$

where $\boldsymbol{\tau}$ is the tangent vector to Γ , whereas $h_{(\Gamma)}$ is a given function defined on the boundary (Agoshkov and Saleri, 1996).

From the mathematical standpoint unforced inviscid SWEs are based on several conservation laws. In particular, the mass

$$M(t) = \int_D H dD, \quad (7)$$

the total energy

$$E(t) = \frac{1}{2} \int_D [(u^2 + v^2)H + g(h^2 - h_T^2)] dD \quad (8)$$

and the potential enstrophy

$$J(t) = \frac{1}{2} \int_D H \left(\frac{\zeta + f}{H} \right)^2 dD, \quad (9)$$

where

$$\zeta = \frac{1}{R \cos \varphi} \left(\frac{\partial v}{\partial \lambda} - \frac{\partial u \cos \varphi}{\partial \varphi} \right), \quad (10)$$

are kept constant in time for a closed shallow-water system (Vreugdenhil, 1994; Kundu et al., 2012). In the numerical simulation of shallow-water flows one should use the finite difference schemes which preserve the discrete analogues of the integral invariants of motion (7)-(9) as accurately as possible. It is crucial that for many finite difference schemes the discrete analogues of the mass, total energy and potential enstrophy are usually not invariant in time, so the numerical method can be unstable and the resulting simulation becomes inaccurate (Vreugdenhil, 1994). This emphasises the importance of using conservative difference schemes while modelling fluid dynamics phenomena.

In the last forty years there have been suggested several finite difference schemes that conserve some or other integral characteristics of the shallow-water equations (Sadourny, 1975; Arakawa and Lamb, 1981; Heikes and Randall, 1995; Ringler and Randall, 2002; Bouchut et al., 2004; LeVeque and George, 2007; Salmon, 2009). In all these works, however, only semi-discrete (i.e., discrete only in space, but still continuous in time) conservative schemes are constructed. After using an explicit time discretisation those schemes stop being conservative. Besides, while aiming to achieve the desired full conservativeness (see, e.g., (Shokin, 1988)), when all the discrete analogues of the integral invariants of motion are conserved, some methods require rather complicated spatial grids (e.g., triangular, hexagonal, etc.), which makes it difficult to employ those methods in a computational domain with a boundary of an arbitrary shape; alternatively, it may result in a resource-intensive numerical algorithm.

In this work we suggest a new efficient method for the numerical simulation of shallow-water flows in domains of complex geometries. The method is based on our earlier research devoted to the modelling of atmospheric waves with SWEs (Skiba, 1995; Skiba and Filatov, 2008; Skiba and Filatov, 2009). The method involves operator splitting of the original equations by physical processes and by coordinates. Careful subsequent discretisation of the split 1D systems coupled with the Crank-Nicolson approximation of the spatial terms yields a fully discrete (i.e., discrete both in time and in space) finite difference shallow-water model that, in case of an inviscid and unforced fluid, exactly conserves the mass and the total energy, while the potential enstrophy is bounded, oscillating in time within a narrow band. Due to the prior splitting the model is extremely efficient, since

it is implemented as systems of linear algebraic equations with tri- and five-diagonal matrices. Furthermore, the model can straightforwardly be realised on high-performance parallel computers without any significant modifications in the original single-threaded algorithm.

The paper is organised as follows. In Section 2 we give the mathematical foundations of the suggested shallow-water model. In Section 3 we test the model with several numerical experiments aimed to simulate shallow-water flows in a bay-like domain with a complex boundary. We also test a modified model, taking into account fluid viscosity and external forcing for providing more realistic simulation. In Section 4 we give a conclusion.

2 FULLY DISCRETE MASS - AND ENERGY - CONSERVING SHALLOW-WATER MODEL

Rewrite the shallow-water equations (1)-(3) in the operator form

$$\frac{\partial \vec{\psi}}{\partial t} + \mathbf{A}(\vec{\psi}) = 0, \quad (11)$$

where $\mathbf{A}(\vec{\psi})$ is the shallow-water nonlinear operator, while $\vec{\psi} = (U, V, h\sqrt{g})^T$ is the unknown vector. Now represent the operator $\mathbf{A}(\vec{\psi})$ as a sum of three simpler operators, nonlinear \mathbf{A}_1 , \mathbf{A}_2 and linear \mathbf{A}_3

$$\mathbf{A}(\vec{\psi}) = \mathbf{A}_1(\vec{\psi}) + \mathbf{A}_2(\vec{\psi}) + \mathbf{A}_3\vec{\psi}. \quad (12)$$

Let (t_n, t_{n+1}) be a sufficiently small time interval with a step τ ($t_{n+1} = t_n + \tau$). Applying in (t_n, t_{n+1}) operator splitting to (11), we approximate it by the three simpler problems

$$\frac{\partial \vec{\psi}_1}{\partial t} + \mathbf{A}_1(\vec{\psi}_1) = 0, \quad (13)$$

$$\frac{\partial \vec{\psi}_2}{\partial t} + \mathbf{A}_2(\vec{\psi}_2) = 0, \quad (14)$$

$$\frac{\partial \vec{\psi}_3}{\partial t} + \mathbf{A}_3\vec{\psi}_3 = 0. \quad (15)$$

According to the method of splitting, these problems are to be solved one after another, so that the solution to (11) from the previous time interval (t_{n-1}, t_n) is the initial condition for (13): $\vec{\psi}_1(t_n) = \vec{\psi}(t_n)$, then $\vec{\psi}_2(t_n) = \vec{\psi}_1(t_{n+1})$ and finally $\vec{\psi}_3(t_n) = \vec{\psi}_2(t_{n+1})$. Therefore, the solution to (11) at the moment t_{n+1} is approximated by the solution $\vec{\psi}_3(t_{n+1})$ (Marchuk, 1982).

Operators \mathbf{A}_1 , \mathbf{A}_2 , \mathbf{A}_3 can be defined in different ways. In our work equation (13) has the form

$$\begin{aligned} \frac{\partial U}{\partial t} + \frac{1}{R \cos \varphi} \frac{1}{2} \left[\frac{\partial u U}{\partial \lambda} + u \frac{\partial U}{\partial \lambda} \right] \\ = - \frac{gz}{R \cos \varphi} \frac{\partial h}{\partial \lambda}, \end{aligned} \quad (16)$$

$$\frac{\partial V}{\partial t} + \frac{1}{R \cos \varphi} \frac{1}{2} \left[\frac{\partial v U}{\partial \lambda} + u \frac{\partial V}{\partial \lambda} \right] = 0, \quad (17)$$

$$\frac{\partial h}{\partial t} + \frac{1}{R \cos \varphi} \frac{\partial z U}{\partial \lambda} = 0, \quad (18)$$

for (14) we take

$$\frac{\partial U}{\partial t} + \frac{1}{R \cos \varphi} \frac{1}{2} \left[\frac{\partial v U \cos \varphi}{\partial \varphi} + v \cos \varphi \frac{\partial U}{\partial \varphi} \right] = 0, \quad (19)$$

$$\begin{aligned} \frac{\partial V}{\partial t} + \frac{1}{R \cos \varphi} \frac{1}{2} \left[\frac{\partial v V \cos \varphi}{\partial \varphi} + v \cos \varphi \frac{\partial V}{\partial \varphi} \right] \\ = - \frac{gz}{R} \frac{\partial h}{\partial \varphi}, \end{aligned} \quad (20)$$

$$\frac{\partial h}{\partial t} + \frac{\partial z V \cos \varphi}{\partial \varphi} = 0, \quad (21)$$

and for (15) —

$$\frac{\partial U}{\partial t} - \left(f + \frac{u}{R} \tan \varphi \right) V = 0, \quad (22)$$

$$\frac{\partial V}{\partial t} + \left(f + \frac{u}{R} \tan \varphi \right) U = 0. \quad (23)$$

This choice of \mathbf{A}_i 's corresponds to the splitting by physical processes (transport and rotation) and by coordinates (λ and φ). The latter means that while solving (16)-(18) in λ , the coordinate φ is left fixed; and vice versa for (19)-(21).

Introducing the grid $\{(\lambda_k, \varphi_l) \in D : \lambda_{k+1} = \lambda_k + \Delta\lambda, \varphi_{l+1} = \varphi_l + \Delta\varphi\}$, we approximate systems (16)-(18) and (19)-(21) by the central second-order finite difference schemes, so that eventually in λ we obtain (the subindex l , in the φ -direction, is fixed, as well as omitted for simplicity)

$$\begin{aligned} \frac{U_k^{n+1} - U_k^n}{\tau} + \frac{1}{2c_l} \left[\frac{\bar{u}_{k+1} U_{k+1} - \bar{u}_{k-1} U_{k-1}}{2\Delta\lambda} \right. \\ \left. + \bar{u}_k \frac{U_{k+1} - U_{k-1}}{2\Delta\lambda} \right] \\ = - \frac{g\bar{z}_k}{c_l} \frac{h_{k+1} - h_{k-1}}{2\Delta\lambda}, \end{aligned} \quad (24)$$

$$\begin{aligned} \frac{V_k^{n+1} - V_k^n}{\tau} + \frac{1}{2c_l} \left[\frac{\bar{u}_{k+1} V_{k+1} - \bar{u}_{k-1} V_{k-1}}{2\Delta\lambda} \right. \\ \left. + \bar{u}_k \frac{V_{k+1} - V_{k-1}}{2\Delta\lambda} \right] = 0, \end{aligned} \quad (25)$$

$$\frac{h_k^{n+1} - h_k^n}{\tau} + \frac{1}{c_l} \frac{\bar{z}_{k+1} U_{k+1} - \bar{z}_{k-1} U_{k-1}}{2\Delta\lambda} = 0, \quad (26)$$

while in φ we get (the subindex k , in λ , is fixed and omitted too)

$$\frac{U_l^{n+1} - U_l^n}{\tau} + \frac{1}{2c_l} \left[\frac{\bar{v}_{l+1}U_{l+1}c_+ - \bar{v}_{l-1}U_{l-1}c_-}{2\Delta\varphi} + \bar{v}_l \cos\varphi_l \frac{U_{l+1} - U_{l-1}}{2\Delta\varphi} \right] = 0, \quad (27)$$

$$\frac{V_l^{n+1} - V_l^n}{\tau} + \frac{1}{2c_l} \left[\frac{\bar{v}_{l+1}V_{l+1}c_+ - \bar{v}_{l-1}V_{l-1}c_-}{2\Delta\varphi} + \bar{v}_l \cos\varphi_l \frac{V_{l+1} - V_{l-1}}{2\Delta\varphi} \right] = -\frac{g\bar{z}_l}{R} \frac{h_{l+1} - h_{l-1}}{2\Delta\varphi}, \quad (28)$$

$$\frac{h_l^{n+1} - h_l^n}{\tau} + \frac{1}{c_l} \frac{\bar{z}_{l+1}V_{l+1}c_+ - \bar{z}_{l-1}V_{l-1}c_-}{2\Delta\varphi} = 0. \quad (29)$$

Here, in a standard manner, $w_{kl}^n = w(\lambda_k, \varphi_l, t_n)$, where $w = \{U, V, h\}$; besides, we denoted $c_l \equiv R \cos\varphi_l$ and $c_{\pm} \equiv \cos\varphi_{l\pm 1}$. In turn, the rotation problem (22)-(23) has the form

$$\frac{U_{kl}^{n+1} - U_{kl}^n}{\tau} - \left(f_l + \frac{\bar{u}_{kl}}{R} \tan\varphi_l \right) V_{kl} = 0, \quad (30)$$

$$\frac{V_{kl}^{n+1} - V_{kl}^n}{\tau} + \left(f_l + \frac{\bar{u}_{kl}}{R} \tan\varphi_l \right) U_{kl} = 0. \quad (31)$$

The functions U_{kl} , V_{kl} in the presented schemes are defined via the Crank-Nicolson approximation as $U_{kl} = (U_{kl}^n + U_{kl}^{n+1})/2$, $V_{kl} = (V_{kl}^n + V_{kl}^{n+1})/2$. As for the overlined functions \bar{u}_{kl} , \bar{v}_{kl} and \bar{z}_{kl} , they can be chosen in an arbitrary manner (Skiba, 1995). For instance, the choice $\bar{w}_{kl} = w_{kl}^n$, where $w = \{u, v, z\}$, will yield linear second-order finite difference schemes, whereas the choice $\bar{w}_{kl} = w_{kl}$ coupled with the corresponding Crank-Nicolson approximations for w_{kl} will produce nonlinear schemes.

The developed schemes have several essential advantages.

First, the coordinate splitting allows simple parallelisation of the numerical algorithm without any significant modifications of the single-threaded code. Indeed, say, when solving (24)-(26), all the calculations along the longitude at different φ_l 's can be done in parallel; analogously, for (27)-(29) the calculations at different λ_k 's are naturally parallelisable. Finally, equations (30)-(31) can be reduced to explicit formulas with respect to U_{kl}^{n+1} , V_{kl}^{n+1} (Skiba and Filatov, 2008).

Second, the simple 1D longitudinal and latitudinal spatial stencils used do not impose any restrictions on the shape of the boundary Γ . Therefore, the developed schemes can be employed for the simulation

of shallow-water flows in computational domains of complex geometries.

Third, the developed schemes are mass- and total-energy-conserving for the inviscid unforced shallow-water model in a closed basin ($\Gamma = \Gamma_c$). To show this, consider, e.g., (24)-(26). The boundary condition will be $U|_{\Gamma} = 0$, which can be approximated as

$$\frac{1}{2}(U_0 + U_1) = 0, \quad (32)$$

$$\frac{1}{2}(U_K + U_{K+1}) = 0, \quad (33)$$

where the nodes $k = 1$ and $k = K$ are inside the domain D , while the nodes $k = 0$ and $k = K + 1$ are out of D (i.e., fictitious). Multiplying (26) by $\tau R \Delta \lambda$, summing over all the $k = \overline{1, K}$'s and taking into account the boundary conditions (32)-(33), we find that the spatial term vanishes, so that

$$\begin{aligned} M_l^{n+1} &= R \Delta \lambda \sum_k H_{kl}^{n+1} = \dots \\ &= R \Delta \lambda \sum_k H_{kl}^n = M_l^n, \end{aligned} \quad (34)$$

which proves that the mass conserves in λ (at a fixed l). Further, multiplying (24) by $\tau R \Delta \lambda U_{kl}$, (25) by $\tau R \Delta \lambda V_{kl}$ and (26) by $\tau R \Delta \lambda g h_{kl}$, summing over the internal k 's and taking into account (32)-(33), we obtain

$$\begin{aligned} E_l^{n+1} &= R \Delta \lambda \sum_k \frac{1}{2} \left([U_{kl}^{n+1}]^2 + [V_{kl}^{n+1}]^2 \right. \\ &\quad \left. + g \left([h_{kl}^{n+1}]^2 - [h_{T,kl}]^2 \right) \right) = \dots \\ &= R \Delta \lambda \sum_k \frac{1}{2} \left([U_{kl}^n]^2 + [V_{kl}^n]^2 \right. \\ &\quad \left. + g \left([h_{kl}^n]^2 - [h_{T,kl}]^2 \right) \right) = E_l^n, \end{aligned} \quad (35)$$

that is the energy conserves in λ at $\varphi = \varphi_l$ too. Similar results can be obtained with respect to the second coordinate, φ (problem (27)-(29)), while the Coriolis problem (30)-(31) does not affect the conservation laws. Note that to establish both the mass and the energy conservation we used the divergence of the spatial terms in (24)-(26) and (27)-(29) (Shokin, 1988). The conservation of the total energy guarantees that the constructed finite difference schemes are absolutely stable (Marchuk, 1982).

Fourth, from (24)-(26), (27)-(29) it follows that under the choice $\bar{w}_{kl} = w_{kl}^n$, where $w = \{u, v, z\}$, the resulting finite difference schemes are systems of linear algebraic equations with either tri- or five-diagonal matrices. Obviously, fast direct (i.e., non-iterative) linear solvers can be used for their solution (Press et al., 2007), so that the exact conservation of the mass and the total energy will not be violated.

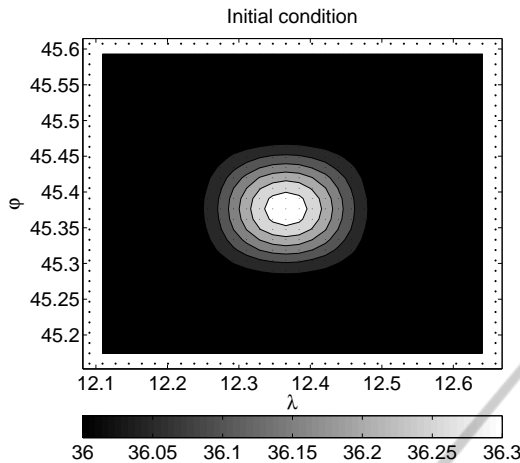


Figure 1: Problem 1, initial condition (the free surface height is shown in meters; the markers ‘.’ denote the fictitious nodes outside the domain).

3 NUMERICAL SIMULATION

For testing the developed model we consider two problems. In the first problem the SWEs are a closed system, so that we are able to verify the mass and the total energy conservation laws; besides, the ranges of the variation of the potential entrophy are analysed. In the second experiment the problem is complicated by introducing a complex boundary with open and closed segments, a nonzero viscosity, as well as a nonzero source function imitating the wind. Such a setup simulates wind-driven shallow-water flows in a bay.

Problem 1. In this experiment we consider the simplest case: for the computational domain we take the spherical rectangle $D = \{(\lambda, \varphi) : \lambda \in (12.10, 12.65), \varphi \in (45.16, 45.60)\}$ with a closed boundary $\Gamma = \Gamma_c$. This will allow to verify whether the mass and the total energy of an inviscid unforced fluid are exactly conserved in the numerical simulation. For the initial velocity field we take $u = v = 0$, while the free surface height is a hat-like function (Fig. 1). The gridsteps are $\Delta\lambda \approx \Delta\varphi \approx 0.015^\circ$, $\tau = 1.44$ min.

In Fig. 2 we plot the graphs of the discrete analogues of invariants (7)-(9). As it is seen, the mass and the total energy are conserved exactly, while the behaviour of the potential entrophy is stable—it is oscillating within a narrow band, with a drastically small maximum relative error about 0.32%, without unbounded growth or decay. This confirms the theoretical calculations (34)-(35), as well as demonstrates that the developed schemes allow obtaining physically adequate simulation results.

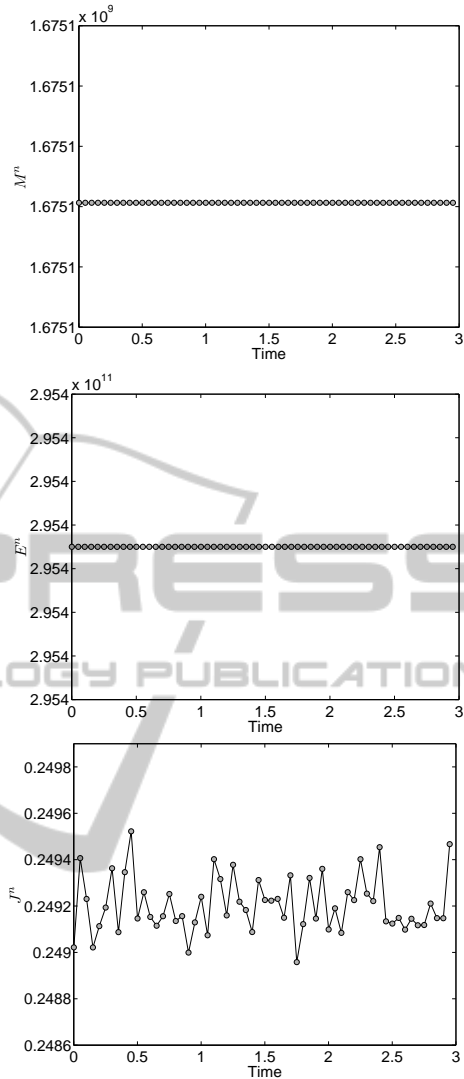


Figure 2: Problem 1, behaviour of the mass, total energy and potential entrophy in time (in days). Maximum relative error of J^n does not exceed 0.32%.

Problem 2. Having a numerical shallow-water model that conserves the mass and the total energy in the absence of sources and sinks of energy, now consider a more complex problem.

For the computational domain we choose the region shown in Fig. 3. Unlike the previous problem, the boundary is now of an arbitrary shape; besides, there are several onshore parts surrounded by water which represent small isles. The boundary Γ is divided into the closed and open segments: $\Gamma_o = \{\lambda \in (12.32, 12.65), \varphi = 45.16\} \cup \{\lambda = 12.65, \varphi \in (45.16, 45.50)\}$, $\Gamma_c = \Gamma \setminus \Gamma_o$. This setup aims to simulate flows that may occur in the Bay of Venice.

In order to make the flows more realistic, terms responsible for fluid viscosity are also added into

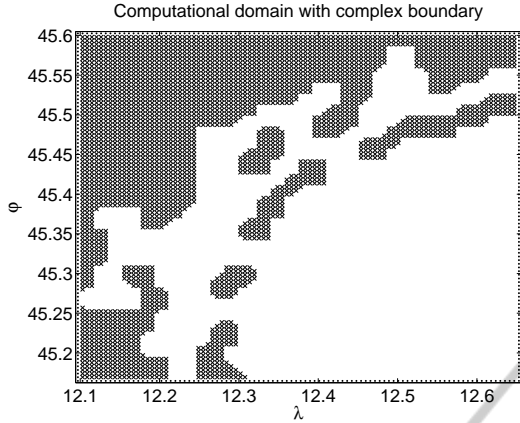


Figure 3: Problem 2, complex computational domain (white area) with onshore parts and interior isles (grey areas).

the first two equations of the shallow-water system. Specifically, on the right-hand side of (11) we add the vector $\mathbf{D}\bar{\psi}$, where

$$\mathbf{D} = \begin{pmatrix} d_{11} & 0 & 0 \\ 0 & d_{22} & 0 \\ 0 & 0 & 0 \end{pmatrix}, \quad (36)$$

where

$$d_{11} = d_{22} = \frac{D}{R^2 \cos^2 \varphi} \frac{\partial^2}{\partial \lambda^2} + \frac{D}{R^2 \cos \varphi} \frac{\partial}{\partial \varphi} \left(\cos \varphi \frac{\partial}{\partial \varphi} \right). \quad (37)$$

Here D is the viscosity coefficient. However, addition of the viscosity terms into (24)-(25) and (27)-(28) requires a modification of boundary conditions (4)-(6). Following (Agoshkov and Saleri, 1996), we use the boundary conditions

$$\mathbf{n} \cdot \mathbf{u} = 0, \quad Dh \frac{\partial \mathbf{u}}{\partial \mathbf{n}} \tau = 0, \quad (38)$$

$$(|\mathbf{n} \cdot \mathbf{u}| - \mathbf{n} \cdot \mathbf{u})(h - h_{(\Gamma)}) = 0, \quad (39)$$

$$Dh \frac{\partial \mathbf{u}}{\partial \mathbf{n}} = 0. \quad (40)$$

Condition (38) is for \mathbf{u} on the closed segment of the boundary (see also (Simonnet et al., 2003)), while (39) and (40) are for h and \mathbf{u} on the open segment, respectively. Condition (39) is supposed to consist of two parts: the first term fires on the outflow (when $|\mathbf{n} \cdot \mathbf{u}| = \mathbf{n} \cdot \mathbf{u}$), whereas the second term is responsible for the inflow ($h_{(\Gamma)}$ is supposed to be given a priori).

Finally, on the right-hand side of (11) we add a wind stress of the form $\mathbf{W}\bar{\psi} \sin 2\pi t$, where

$$\mathbf{W} \sim \begin{pmatrix} -\cos \frac{\pi(\varphi - \varphi_{\min})}{L_\varphi} & 0 & 0 \\ 0 & \cos \frac{\pi(\varphi - \varphi_{\min})}{2L_\varphi} & 0 \\ 0 & 0 & 0 \end{pmatrix}, \quad (41)$$

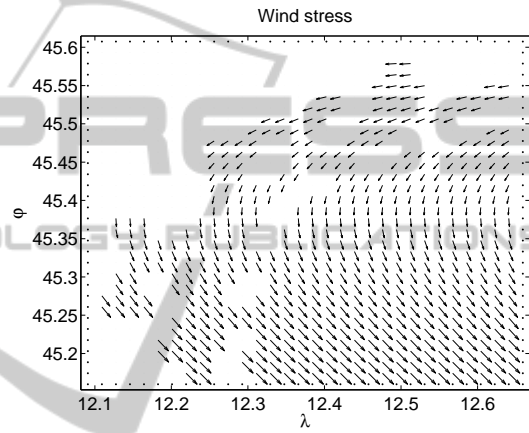
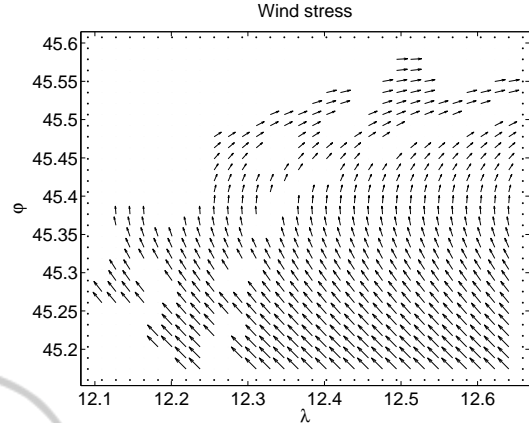


Figure 4: Problem 2, field of the wind stress at $t = 0.25$ (top) and $t = 0.75$ (bottom).

while $L_\varphi = \varphi_{\max} - \varphi_{\min}$. The wind stress field at $t = 0.25$ and $t = 0.75$ is shown in Fig. 4.

The numerical solution computed on the grid $\Delta\lambda \approx \Delta\varphi \approx 0.005^\circ$ and $\tau = 1.44$ min is presented in Fig. 5 at several time moments. Comparison with Fig. 4 shows that a wind-driven flow occurs and is then developing in the computational domain. Specifically, as the simulation starts, the velocity field is formed clockwise (Fig. 5, $t = 0.2, 0.4$), in accordance with the wind stress at small times (Fig. 4, top). Later, at $t = 0.5$, the wind's direction changes to anticlockwise due to the term $\sin 2\pi t$, which is reflected in the numerical solution with a little time gap because of the fluid's inertia, especially in the open ocean far from the coastline: while the coastal waters change their flows at $t \approx 0.5 - 0.7$, the large vortex in the open bay begins rotating anticlockwise at $t \approx 0.8$ (Fig. 5). Finally, at $t = 1$ the entire velocity field is aligned in accordance with the late-time wind stress (Fig. 4, bottom).

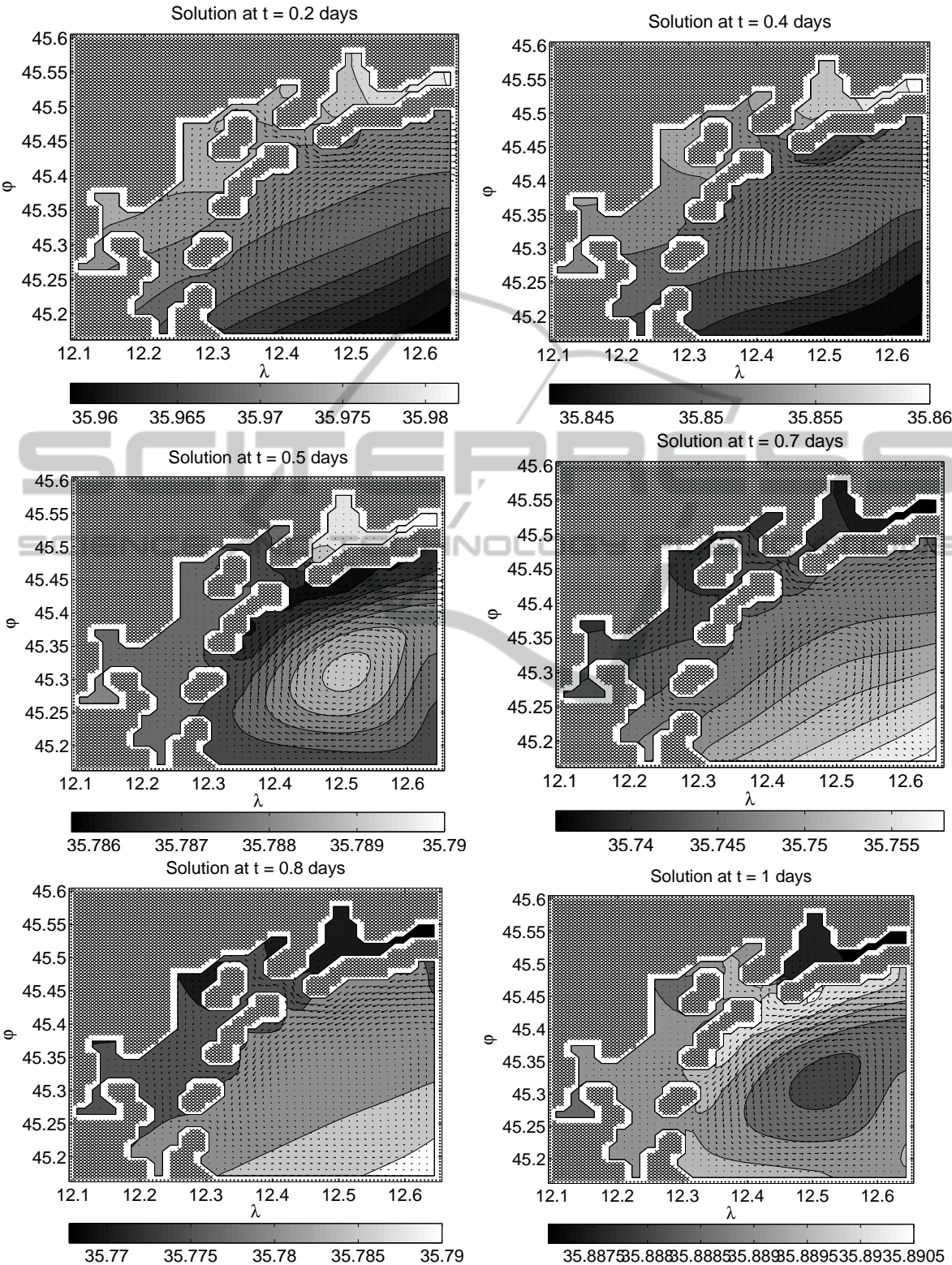


Figure 5: Problem 2, numerical solution at several time moments (the solution is reduced to a coarser grid $\Delta\lambda \approx \Delta\phi \approx 0.01^\circ$ for better visualisation; the fluid's depth is shown by colour, while the velocity field is shown by arrows).

4 CONCLUSIONS

A new fully discrete mass- and total-energy-conserving finite difference model for the simulation of shallow-water flows in bay-like domains with complex boundaries was developed. Having taken the SWEs written in the divergent form, we involved the idea of operator splitting coupled with the Crank-Nicolson approximation and constructed absolutely stable second-order finite difference schemes that allow accurate simulation of shallow-water flows in spherical domains of arbitrary shapes. An important integral invariant of motion of the SWEs, the potential enstrophy, proved to be bounded for an inviscid unforced fluid, oscillating in time within a narrow range. Hence, the numerical solution is mathematically accurate and provides physically adequate results. Due to the method of splitting the developed model can straightforwardly be implemented for distributed simulation of shallow-water flows on high-performance parallel computers. Numerical experiments with a simple inviscid unforced closed shallow-water system and with a viscous open wind-driven shallow-water model simulating a real situation nicely confirmed the skills of the new method.

ACKNOWLEDGEMENTS

This research was partially supported by the grants No. 14539 and No. 26073 of the National System of Researchers of Mexico (SNI), and is part of the projects PAPIIT-UNAM IN104811 and PAPIME-UNAM PE103311, Mexico.

REFERENCES

- Agoshkov, V. I. and Saleri, F. (1996). Recent developments in the numerical simulation of shallow water equations. part iii: Boundary conditions and finite element approximations in the river flow calculations. *Math. Modelling*, 8:3–24.
- Arakawa, A. and Lamb, V. R. (1981). A potential enstrophy and energy conserving scheme for the shallow-water equation. *Mon. Wea. Rev.*, 109:18–36.
- Bouchut, F., Sommer, J. L., and Zeitlin, V. (2004). Frontal geostrophic adjustment and nonlinear wave phenomena in one-dimensional rotating shallow water. part ii: High-resolution numerical simulations. *J. Fluid Mech.*, 514:35–63.
- Heikes, R. and Randall, D. A. (1995). Numerical integration of the shallow-water equations on a twisted icosahedral grid. part i: Basic design and results of tests. *Mon. Wea. Rev.*, 123:1862–1880.
- Jirka, G. H. and Uijttewaal, W. S. J., editors (2004). *Shallow Flows*, London. Taylor & Francis.
- Kundu, P. K., Cohen, I. M., and Dowling, D. R. (2012). *Fluid Mechanics*. Academic Press, 5th edition.
- LeVeque, R. J. and George, D. L. (2007). High-resolution finite volume methods for the shallow-water equations with bathymetry and dry states. In Yeh, H., Liu, P. L., and Synolakis, C. E., editors, *Advanced Numerical Models for Simulating Tsunami Waves and Runup*, pages 43–73. World Scientific Publishing, Singapore.
- Marchuk, G. I. (1982). *Methods of Computational Mathematics*. Springer-Verlag, Berlin.
- Oliger, J. and Sundstrom, A. (1978). Theoretical and practical aspects of some initial boundary value problems in fluid dynamics. *SIAM J. Appl. Anal.*, 35:419–446.
- Pedlosky, J. (1987). *Geophysical Fluid Dynamics*. Springer, 2nd edition.
- Press, W. H., Teukolsky, S. A., Vetterling, W. T., and Flannery, B. P. (2007). *Numerical Recipes: The Art of Scientific Computing*. Cambridge University Press, Cambridge.
- Ringler, T. D. and Randall, D. A. (2002). A potential enstrophy and energy conserving numerical scheme for solution of the shallow-water equations on a geodesic grid. *Mon. Wea. Rev.*, 130:1397–1410.
- Sadourny, R. (1975). The dynamics of finite-difference models of the shallow-water equations. *J. Atmos. Sci.*, 32:680–689.
- Salmon, R. (2009). A shallow water model conserving energy and potential enstrophy in the presence of boundaries. *J. Mar. Res.*, 67:1–36.
- Shokin, Y. I. (1988). Completely conservative difference schemes. In de Vahl Devis, G. and Fletcher, C., editors, *Computational Fluid Dynamics*, pages 135–155. Elsevier, Amsterdam.
- Simonnet, E., Ghil, M., Ide, K., Temam, R., and Wang, S. (2003). Low-frequency variability in shallow-water models of the wind-driven ocean circulation. part i: Steady-state solution. *J. Phys. Ocean.*, 33:712–728.
- Skiba, Y. N. (1995). Total energy and mass conserving finite difference schemes for the shallow-water equations. *Russ. Meteorol. Hydrology*, 2:35–43.
- Skiba, Y. N. and Filatov, D. M. (2008). Conservative arbitrary order finite difference schemes for shallow-water flows. *J. Comput. Appl. Math.*, 218:579–591.
- Skiba, Y. N. and Filatov, D. M. (2009). Simulation of soliton-like waves generated by topography with conservative fully discrete shallow-water arbitrary-order schemes. *Internat. J. Numer. Methods Heat Fluid Flow*, 19:982–1007.
- Vol'tsynger, N. E. and Pyaskovskiy, R. V. (1977). *Theory of Shallow Water*. Gidrometeoizdat, St. Petersburg.
- Vreugdenhil, C. B. (1994). *Numerical Methods for Shallow-Water Flow*. Kluwer Academic, Dordrecht.